Quantitative Orbital Analysis of *Ab Initio* SCF-MO Computations. Part 3.† Torsional Isomerisms in But-2-enes

Fernando Bernardi *
Istituto Chimico G. Ciamician, Via Selmi 2, Università di Bologna, Bologna, Italy
Andrea Bottoni
Istituto di Chimica Organica, Viale Risorgimento 4, Università di Bologna, Bologna, Italy
Glauco Tonachini
Istituto di Chimica Organica, Via Bidone 36, Università di Torino, Torino, Italy

We describe the results obtained from quantitative orbital analysis, using *ab initio* SCF-MO computations, of the torsional isomerism of but-2-ene. The analysis is based on the use of σ fragment localized MOs and π fragment canonical MOs and the energy effects associated with their interactions are estimated using the quantitative Perturbational Molecular Orbital (PMO) and Total Energy approaches. It is found that conformational preferences in both *cis*- and *trans*-but-2-ene are determined by the π non-bonded interactions under matrix element control, while the trend in the relative stability of the two stable geometric isomers, $t_{ee} > c_{ee}$, is determined mainly by the difference in the steric repulsions between the σ_{CH} bond MOs of the two methyl groups.

In recent papers,[1,2] we have described a procedure which provides estimates, in the framework of an *ab initio* SCF-MO computation, of the energy effects associated with various types of interactions occurring between the component fragments of a closed shell molecule. These interactions involve Coulomb and orbital interactions. The energy effects associated with the Coulomb interactions are simply estimated using the net charges taken from the results of the Mulliken population analysis, while those associated with the orbital interactions are computed in terms of SCF-MO total energy values obtained in the absence of the interactions under examination (Total Energy approach) and also in terms of Perturbational MO expressions [3,4] (PMO approach). We have suggested that the combined use of these two types of quantitative analysis provides a better understanding of the role played by the various factors which control a structural problem.[1]

This computational procedure is applied here to the analysis of the factors which control conformational and geometrical isomerism in but-2-ene. For comparative purposes we have extended our analysis to propene, the parent single methyl derivative. In these applications, the effects of the π and σ non-bonded interactions have been analysed separately using, as the basis, σ-type fragment localized MOs and π-type fragment canonical MOs.

The problem of torsional isomerism in but-2-ene has already been analysed in terms of a qualitative PMO approach, coupled with *ab initio* SCF-MO computations.[5] Furthermore, Wolfe *et al.*[6] have recently reported the results of a quantitative orbital analysis including only π orbitals, where they have attempted to rationalize the order of stability of the three stable isomers of dimethylethylene (1,1, *cis*-1,2, and *trans*-1,2) in terms of the energy effects associated with the π non-bonded interactions. Therefore this paper also serves to demonstrate the advantages of using a complete quantitative treatment for analysing a structural problem which includes all the energy effects associated with all the interactions occurring between the valence MOs of the interacting fragments, over a qualitative or an incomplete quantitative approach.

† Part 2, F. Bernardi, A. Bottoni, A. Mangini, and G. Tonachini, *J. Mol. Struct., Theochem.*, 1981, **86**, 163.

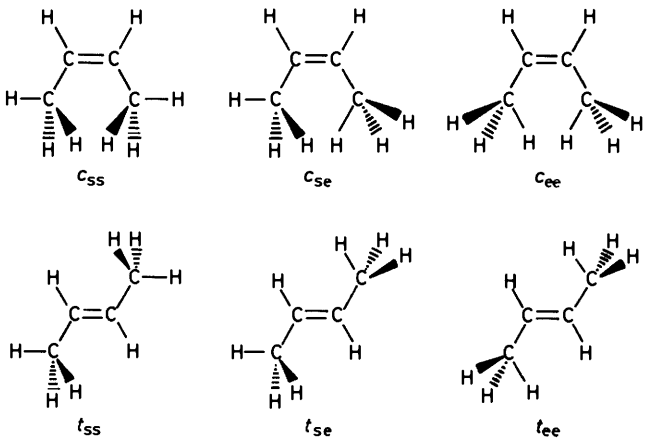

Methods

The *ab initio* SCF-MO computations and associated quantitative analyses have been carried out at the STO-3G level [7] for the staggered and eclipsed conformations of propene and for six conformations of but-2-ene. In this paper we denote as staggered (s) the conformation of a propene where the in-plane hydrogen of a methyl group is staggered relative to the double bond. Similar definition holds for the eclipsed (e) conformation. Accordingly the labels c_{ss} and t_{ss} correspond to the *cis*- and *trans*-but-2-ene where the two component propene fragments both adopt a staggered conformation. Similar definitions hold for the other labels.

The SCF values have been computed with the Gaussian 76 series of programs [8] and in all cases the computations were performed at optimized geometries: for propene we used geometries fully optimized at the STO-3G level,[9] while for but-2-ene we used the STO-4G optimized geometries previously reported.[5]

Propene and but-2-ene (c_{ss} form) have been dissected as shown in Scheme 1.

The MOs of the various basic fragments have been obtained in the following way:

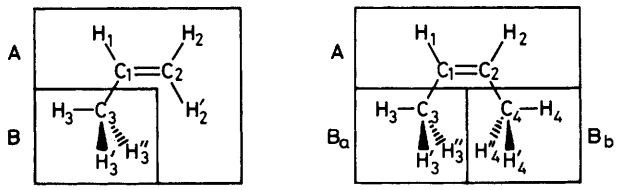

Scheme 1

and $\pi^*_{CH_3}$). The resulting MOs used for the CH_3 fragment are illustrated in Figure 1 in order of increasing energy. The whole procedure provides a set of fragment MOs where all the MOs now have correct orbital occupancies.

(ii) $CH{=}CH_2$ *and* $CH{=}CH$ *Fragments.*—For these fragments we left unchanged the fragment canonical π MOs and we localized only the fragment canonical σ MOs. The resulting valence MOs are illustrated in Figure 1 in order of increasing

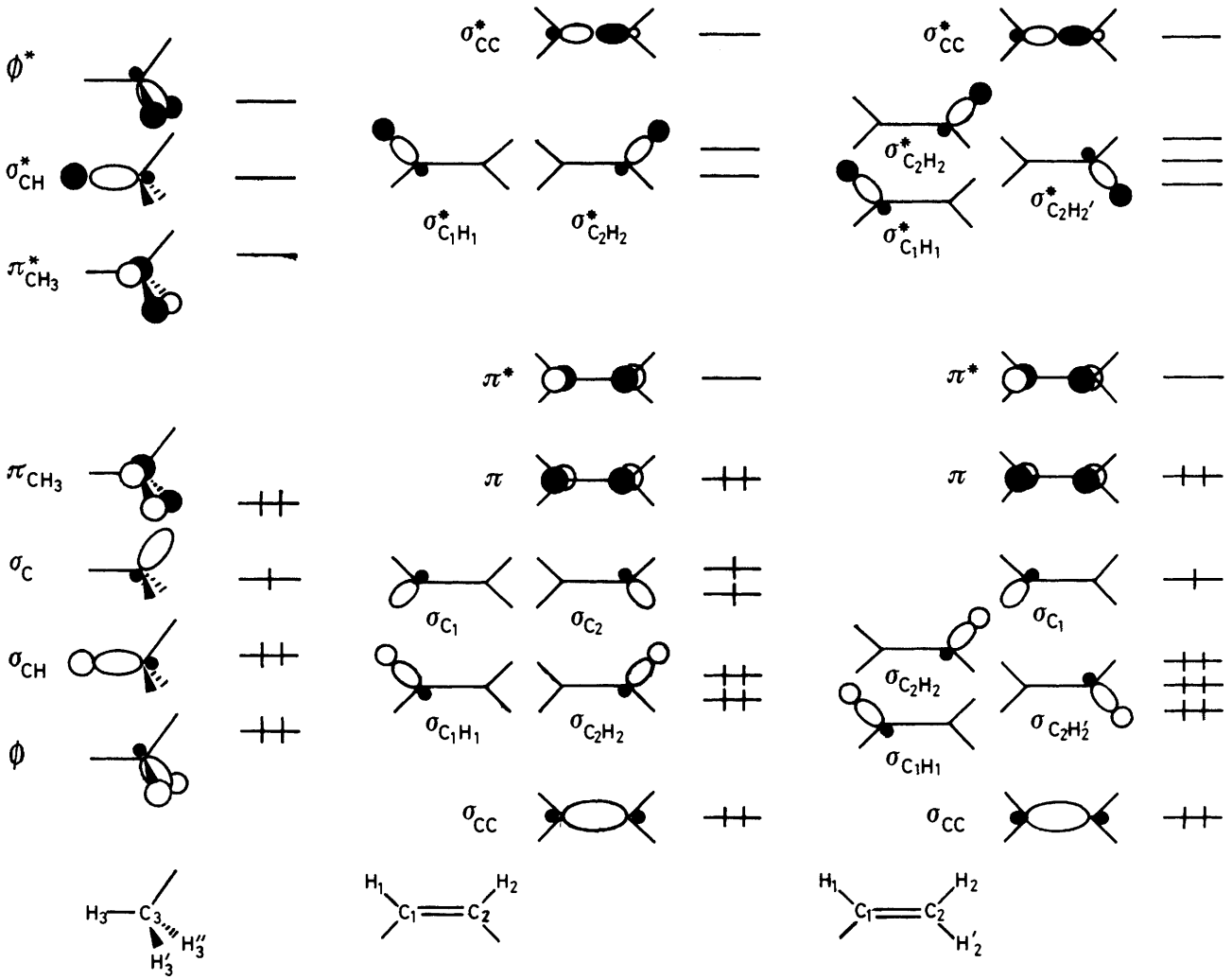

Figure 1. MOs of the various basic fragments CH_3, $CH{=}CH$, and $CH{=}CH_2$

(i) H_3C *Fragment.*—We first computed the localized MOs for each H_3C fragment with the procedure recently suggested.[1,2] This procedure provides the following valence localized MOs: three almost degenerate doubly occupied σ MOs localized along the three C–H bonds and bonding between C and H (the σ_{CH} bond MOs), a singly occupied σ MO localized along the C–C axis and pointing towards the adjacent fragment (σ_C), and three almost degenerate vacant σ MOs localized along the three C–H bonds and antibonding between C and H (the σ_{CH}* antibond MOs). We then diagonalized the submatrix of the Fock matrix expressed in the fragment localized basis, associated only with the out-of-plane σ_{CH} and σ_{CH}* MOs. From this diagonalization we obtain a doubly occupied and a vacant σ-type MO (φ and φ^*) and a doubly occupied and a vacant canonical π-type MO (π_{CH_3} energy. Therefore the $CH{=}CH_2$ fragment involves a doubly occupied σ MO localized along the C–C axis and bonding between the two carbon atoms (σ_{CC}), three doubly occupied σ MOs localized along the three C–H bonds and bonding between C and H (σ_{CH}), a singly occupied σ MO localized along the C(1)–C(3) axis and pointing toward the CH_3 fragment [$\sigma_{C(1)}$], a doubly occupied π MO (π), a vacant π MO (π^*), three vacant σ MOs localized along the three C–H bonds and antibonding between C and H (σ_{CH}*), and a vacant σ MO localized along the C–C axis and antibonding between the two carbon atoms (σ_{CC}*). The MOs of the $CH{=}CH$ fragment are similar to those just described for the $CH{=}CH_2$ fragments: the only differences concern the number of σ_{CH}, σ^*_{CH}, and σ_C, which in this case are two for each type of MO.

These fragment MOs allow us to discuss separately the con-

tribution of the σ-type and π-type interactions. The energy effects associated with the various orbital interactions are computed here in terms of a quantitative PMO treatment: their combined use provides, in fact, a better understanding of the role played by the various factors which control a structural problem.

Total Energy Approach.—We carried out the following calculations of the total energy using the dissection shown in Scheme 1: (a) calculations where the π interactions between the fragments A and B in propene and between the fragments A, B_a, and B_b in but-2-ene are decoupled (complete decoupling); (b) calculations for but-2-ene where only the interactions between the fragments A and B are decoupled, but not those between the sub-fragments B_a and B_b (partial decoupling).

From the results of such computations, an index of energy effects associated with the π interactions under examination can be derived [equation (1) where E_T denotes the total

$$I_A = E_T - E_T^0 \quad (1)$$

energy of the system computed by the SCF method and E_T^0 the total energy of the system in the absence of the π interactions under examination]. This value represents an estimate of the overall energy effect associated with the π orbital interactions of interest. We also denote with E_T^0 the total energy in the case of complete decoupling and with $E_T^{0\prime}$ the corresponding quantity in the case of partial decoupling. We therefore denote with $I_A = E_T - E_T^0$ the overall energy effect, with $I_A' = E_T^{0\prime} - E_T^0$ the energy effect associated just with π interactions occurring between the subfragments B_a and B_b, and with $I_A'' = E_T - E_T^{0\prime}$ the energy effect associated with π interactions occurring between the fragments A and B.

Furthermore, the comparative analysis of the total energy values in the absence of the π interactions provides information about the relative importance of the energy effects associated with σ interactions.

PMO Approach.—In the quantitative PMO treatment, the interaction energy which obtains in the union of the component fragments is estimated on the basis of expression (2)

$$\Delta E = \Sigma\Delta E^4_{ij} + \Sigma\Delta E^2_{ij} + E_c \quad (2)$$

where equations (3)—(5) hold. ΔE^4_{ij} represents the destabilization energy associated with the interaction between two

$$\Delta E^4_{ij} = 4(\varepsilon_0 S^2_{ij} - H_{ij}S_{ij})/(1 - S^2_{ij}) \quad (3)$$

$$\Delta E^2_{ij} = 2(H_{ij} - S_{ij}\varepsilon_i)^2/(\varepsilon_i - \varepsilon_j) \quad (4)$$

$$E_c = \sum_{r<r'} q_r q_{r'}/R_{rr'} \quad (5)$$

doubly occupied MOs φ_i and φ_j, ΔE^2_{ij} the stabilization energy associated with the interaction between a doubly occupied MO φ_i and a vacant MO φ_j, and E_c the coulomb energy associated with the interaction of the component fragments, where q_r denotes the net atomic charge on atom r and $R_{rr'}$ the distance between atoms r and r'. In expressions (3) and (4), ε_i and ε_j denote the energies of the unperturbed MOs φ_i and φ_j, S_{ij} their overlap integral, H_{ij} their matrix element, and ε_0 the mean of the energies ε_i and ε_j. Equation (3) is obtained by application of the variation method to the case of a two-orbital interaction problem,[10] while equation (4) is a well known result of perturbation theory.[11] The various terms in these expressions are then computed using the results of the *ab initio* SCF-MO computations, as recently suggested.[1,2]

Table 1. Total energies (a.u.) of the staggered and eclipsed conformations of propene with (E_T) and without (E_T^0) π interactions, computed at the STO-3G level, together with the index I_A (kcal mol^{-1})

	Staggered		
	Optimized geometry	Rigid geometry	Eclipsed
E_T	−115.657 85	−115.657 78	−115.660 30
E_T^0	−115.679 52	−115.679 90	−115.679 71
I_A	13.60	13.88	12.18

Results and Discussion

We have recently suggested [1,2] that for analysing structural problems in terms of the quantitative PMO analysis it is convenient to perform first a quantitative analysis of a rigid model, followed by additional quantitative analysis of the effects of geometry relaxation. Consequently, for propene, we have performed the quantitative analysis at the eclipsed optimized geometry, at the staggered geometry obtained through a rigid rotation of the eclipsed geometry (staggered rigid geometry), and at the staggered optimized geometry. For the comparison between *cis*- and *trans*-but-2-ene, we have performed the quantitative analysis at the t_{ee} optimized geometry, at the c_{ee} geometry obtained through rigid rotation of the t_{ee} geometry, and at the c_{ee} optimized geometry, while for the comparison between cisoid and transoid conformers, we have compared the optimized geometries, since they do not differ significantly.

Conformational Isomerism of Propene.—The total energy values computed for the various conformations of propene with (E_T) and without (E_T^0) the π interactions are listed in Table 1. Therefore, propene is found, at the STO-3G level, to be more stable in the eclipsed geometry in agreement with the experimental evidence: the computed energy difference between the two conformers is 1.58 kcal mol^{-1} in the rigid model and 1.53 kcal mol^{-1} in the optimized model, values which agree well with the experimental rotational barrier of 2.00 kcal mol^{-1}.[12] However, in the absence of the π interactions, the total energy values of the two conformers become almost identical. This result is indicative of the critical importance of such interactions in determining the conformational preference and the order of magnitude of the rotational barrier in propene. The overall energy effect associated with these π interactions (see the I_A values in Table 1) is destabilizing, and less destabilizing in the eclipsed geometry.

The results of the quantitative PMO analysis are listed in Table 2, while the corresponding interaction diagram is shown in Figure 2. We discuss first the results obtained in the rigid model. The overall energy effect associated with the non-bonded interactions ($\Sigma\Delta E$) is destabilizing and less destabilizing in the eclipsed than in the staggered geometry. Therefore the trend of the overall energy effect parallels the total energy behaviour. Also the $\Sigma\Delta E$ difference for the two geometries (1.03 kcal mol^{-1}) agrees well with the total energy difference. Both the σ and π components of the overall energy effect [$\Sigma\Delta E(\sigma)$ and $\Sigma\Delta E(\pi)$] are destabilizing. However, while $\Sigma\Delta E(\sigma)$ slightly favours the staggered geometry, $\Sigma\Delta E(\pi)$ favours the eclipsed geometry by a larger amount and therefore dictates the conformational preference. It can also be observed that the energy effect associated with the π non-bonded interactions computed with the PMO analysis [$\Sigma\Delta E(\pi)$] agrees well in trend and magnitude with that computed by the Total Energy approach.

Table 2. Energy effects (kcal mol^{-1}) associated with the relevant orbital interactions occurring in the eclipsed and staggered conformations of propene, computed at the STO-3G level, together with the Coulomb energies (E_c)

	Staggered		
	Optimized geometry	Rigid geometry	Eclipsed
$\Delta E^4_{\varphi\sigma_{C(1)C(2)}}$	1.34	1.35	1.38
$\Delta E^4_{\varphi\sigma_{C(1)H(1)}}$	0.86	0.83	3.69
$\Delta E^4_{\varphi\sigma_{C(2)H(2)}}$	0.00	0.00	0.07
$\Delta E^4_{\varphi\sigma_{C(2)H'(2)}}$	0.49	0.48	0.17
$\Delta E^4_{\sigma_{C(3)H(3)}\sigma_{CC}}$	3.07	3.14	3.15
$\Delta E^4_{\sigma_{C(3)H(3)}\sigma_{C(1)H(1)}}$	6.25	6.55	3.20
$\Delta E^4_{\sigma_{C(3)H(3)}\sigma_{C(2)H(2)}}$	0.10	0.10	0.03
$\Delta E^4_{\sigma_{C(3)H(3)}\sigma_{C(2)H'(2)}}$	0.32	0.32	1.42
$\Sigma\Delta E^4(\sigma)$ [a]	12.42	12.76	13.11
$\Sigma\Delta E^2(\sigma)$ [b]	−1.11	−1.11	−1.14
$\Sigma\Delta E(\sigma)$ [c]	11.31	11.65	11.97
$\Delta E^4_{\pi_{CH_3}\pi}$	14.93	15.26	14.48
$\Delta E^2_{\pi_{CH_3}\pi^*}$	−2.66	−2.75	−2.92
$\Delta E^2_{\pi\pi^*_{CH_3}}$	−1.58	−1.58	−1.98
$\Sigma\Delta E^2(\pi)$	−4.24	−4.33	−4.90
$\Sigma\Delta E(\pi)$ [d]	10.69	10.93	9.58
$\Sigma\Delta E$ [e]	22.00	22.58	21.55
E_c [f]	0.56	0.50	0.51

[a] Total destabilizing energy effect associated with the σ orbital interactions. [b] Total stabilizing energy effect associated with the σ orbital interactions. [c] $\Sigma\Delta E(\sigma) = \Sigma\Delta E^4(\sigma) + \Sigma\Delta E^2(\sigma)$. [d] $\Sigma\Delta E(\pi) = \Sigma\Delta E^4_{\pi_{CH_3}\pi} + \Sigma\Delta E^2(\pi)$. [e] $\Sigma\Delta E = \Sigma\Delta E(\sigma) + \Sigma\Delta E(\pi)$. [f] kcal mol^{-1}.

The detailed analysis of the energy effects associated with the various σ interactions shows that only a few bond–bond repulsions have significant effects and among these the largest differential effects in the two geometries are given by the $\sigma_{C(3)H(3)}$–$\sigma_{C(1)H(1)}$ interaction which favours the eclipsed conformation and by the φ–$\sigma_{C(1)H(1)}$ and the $\sigma_{C(3)H(3)}$–$\sigma_{C(2)H'(2)}$ interactions which favour the staggered conformation by a similar amount. On the other hand the analysis of the energy effects associated with the various π interactions agrees with that already reported by Wolfe *et al.*,[13] and confirms the conclusions reached at the qualitative level.[14,15]

The comparison of the previous results with those obtained at the staggered optimized geometry adds little information: the geometry relaxation, in fact, has only small effects and tends slightly to reduce the largest repulsions such as those associated with the $\sigma_{C(3)H(3)}$–σ_{CC} and the $\sigma_{C(3)H(3)}$–$\sigma_{C(1)H(1)}$ interactions.

In Table 2 we have also listed the values of the Coulomb energy (E_c) associated with the interaction of the H_3C and $CH{=}CH_2$ fragments: these values show that this term has a negligible effect.

Therefore the results of the quantitative PMO analysis agree very well with those obtained with the Total Energy approach. Furthermore the combined use of these two types of results provides a detailed understanding of the origin of the various effects.

Conformational Isomerism of But-2-ene.—The total energy values computed for the various conformations of *cis*- and *trans*-but-2-ene with (E_T) and without (E_T^0) the π interactions are listed in Table 3. The analysis of these results provides the following information. (i) The order of stability of the three conformational isomers has been found to be (see the E_T values) ee > se > ss for both the *cis*- and *trans*-but-2-ene. The same order has been found previously at the STO-4G and

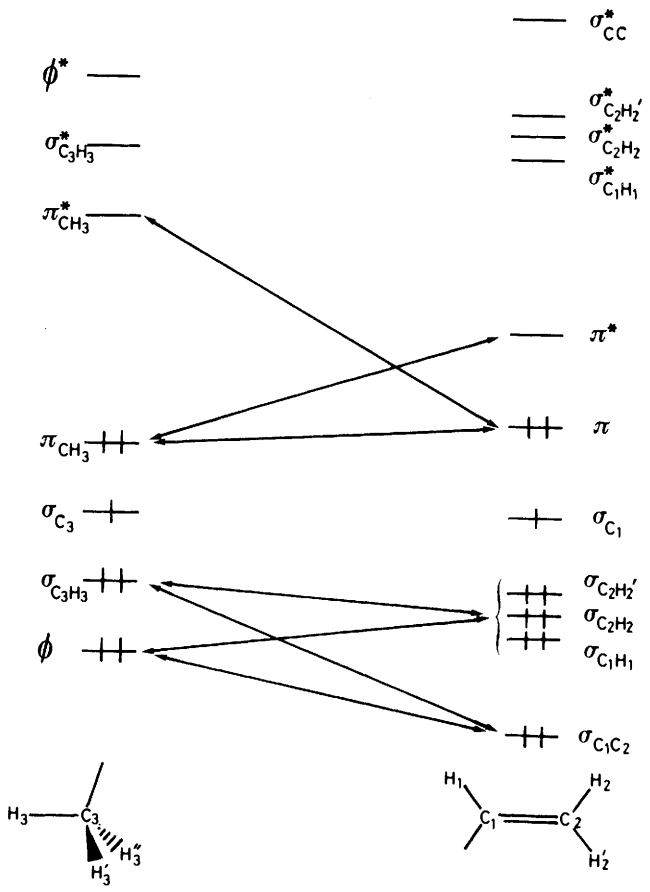

Figure 2. Interaction diagram for propene

at the 4-31G levels.[5] However, in the absence of the π interactions, the order of stability becomes (see the E_T^0 values) ss > se > ee for both the *cis*- and the *trans*-but-2-ene. The differences between the E_T^0 values of the *trans*-conformers are very small (0.14 kcal mol^{-1} between t_{ee} and t_{se} and 0.49 kcal mol^{-1} between t_{se} and t_{ss}), while the corresponding differences between the E_T^0 values of the *cis*-conformers are significantly larger (0.87 kcal mol^{-1} between c_{ee} and c_{se} and 1.17 kcal mol^{-1} between c_{se} and c_{ss}). These results indicate that in *trans*-but-2-ene, the conformational preferences and related energy differences are mainly determined by the π interactions, while in *cis*-but-2-ene even though the conformational trend is again determined by the π interactions, the σ interactions play a significant role in determining the related energy differences.

(ii) The overall energy effect associated with the π interactions (see the I_A values in Table 3) is destabilizing and for these destabilization energies the order ss > se > ee is found for both *cis*- and *trans*-but-2-ene.

(iii) The energy effects associated with the π orbital interactions occurring between the two CH_3 fragments (see the I_A' values in Table 3) are destabilizing, but this term is negligible in all cases except c_{ss}. Therefore the relevant π contribution refers to the interaction between the π MOs of the fragments A and B.

The results of the quantitative PMO analysis are listed in the Tables 4—6, while the appropriate interaction diagrams are shown in Figures 3 and 4. These results agree well with those obtained with the Total Energy approach and also provide a more detailed understanding of the factors determining the various trends. In particular it is found that the

Table 3. Total energies (a.u.) of the various conformations of but-2-ene computed at the STO-3G level with (E_T) and without (E_T^0) π interactions, together with the index I_A (kcal mol^{-1})

	c_{ss}	c_{sc}	c_{ee}	t_{ss}	t_{se}	t_{ee}
E_T	−154.240 64	−154.241 40	−154.241 93 (−154.239 85)	−154.239 93	−154.242 48	−154.244 95
E_T^0	−154.284 93	−154.283 07	−154.281 68 (−154.278 69)	−154.284 92	−154.284 14	−154.283 91
$E_T^{0'}$	−154.283 85	−154.282 93	−154.281 66 (−154.278 66)	−154.284 91	−154.284 13	−154.283 90
I_A	27.79	26.15	24.94 (24.37)	28.23	26.14	24.45
$I_{A'}$	0.68	0.09	0.01 (0.01)	0.01	0.01	0.01
$I_{A''}$	27.11	26.06	24.93 (24.36)	28.22	26.13	24.44

Table 4. Energy effects (kcal mol^{-1}) associated with the relevant orbital interactions occurring between the two H_3C fragments in the various conformations [a] of but-2-ene, computed at the STO-3G level

	c_{ss}	c_{se}	c_{ee} [b]
$\Delta E^4_{\varphi\varphi'}$	1.36	0.01	0.00 (0.00)
$\Delta E^4_{\varphi\sigma'_{CH}}$	0.15	2.34	0.00 (0.00)
$\Delta E^4_{\sigma_{CH}\varphi'}$	0.15	0.00	0.00 (0.00)
$\Delta E^4_{\sigma_{CH}\sigma'_{CH}}$	0.01	0.22	4.96 (9.86)
$\Delta E^2_{\sigma_{CH}\sigma'^*_{CH}}$	0.00	−0.05	−0.09 (−0.20)
$[\Sigma\Delta E^4(\sigma)]_I$	1.67	2.57	4.96 (9.86)
$[\Sigma\Delta E^2(\sigma)]_I$	−0.04	−0.11	−0.26 (−0.54)
$[\Sigma\Delta E(\sigma)]_I$ [c]	1.63	2.46	4.70 (9.32)
$\Delta E^4_{\pi_{CH_3}\pi'_{CH_3}}$	0.50	0.06	0.01 (0.02)
$\Delta E^2_{\pi_{CH_3}\pi'^*_{CH_3}}$	−0.03	0.00	0.00 (0.00)
$\Delta E^2_{\pi'_{CH_3}\pi^*_{CH_3}}$	−0.03	−0.01	0.00 (0.00)
$[\Sigma\Delta E^4(\pi)]_I$	0.50	0.06	0.01 (0.02)
$[\Sigma\Delta E^2(\pi)]_I$	−0.06	−0.01	0.00 (0.00)
$[\Sigma\Delta E(\pi)]_I$ [d]	0.44	0.05	0.01 (0.02)

[a] The corresponding values for the transoid conformations are all less than |0.01| kcal mol^{-1}, and have not been reported here. [b] Values in parentheses refer to results obtained in the rigid model with reference to t_{ee}. [c] $[\Sigma\Delta E(\sigma)]_I = [\Sigma\Delta E^4(\sigma)]_I + [\Sigma\Delta E^2(\sigma)]_I$. [d] $[\Sigma\Delta E(\pi)]_I = [\Sigma\Delta E^4(\pi)]_I + [\Sigma\Delta E^2(\pi)]_I$.

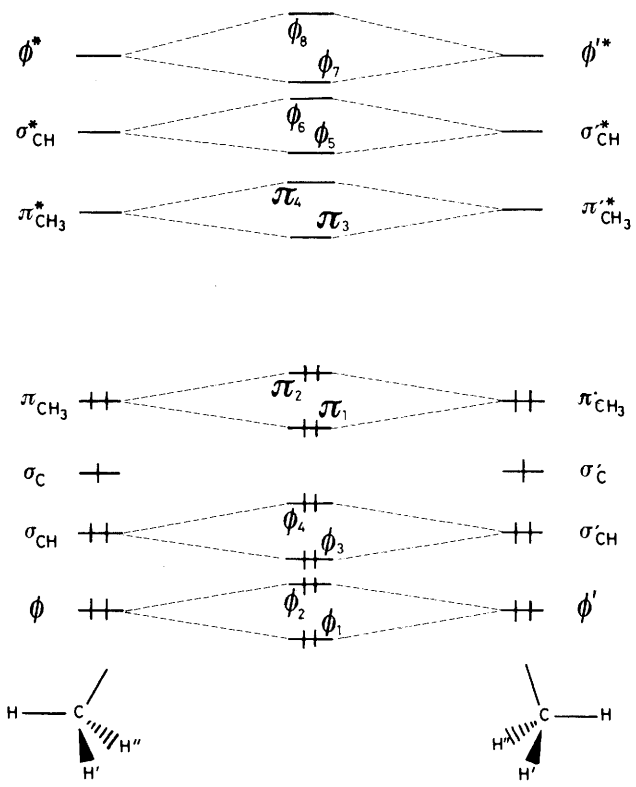

Figure 3. Interaction diagram between two CH_3 fragments in but-2-ene

overall π energy effect, $\Sigma\Delta E(\pi)$, which is destabilizing and agrees well in trend and magnitude with the I_A values, shows the trend ss > se > ee for both *cis*- and *trans*-but-2-ene and therefore parallels the total energy behaviour. On the other hand, the overall σ energy effect, $\Sigma\Delta E(\sigma)$, which is again destabilizing, shows the opposite trend and parallels the behaviour of the total energies computed in the absence of the interactions.

The quantitative PMO approach also provides information about the effects of the various orbital interactions. In particular, for the π orbital interactions, it is found that (i) the energy effects associated with the π orbital interactions occurring between the two CH_3 fragments are negligible in all cases except c_{ss} (see Table 4). Therefore the relevant contributions refer to the interaction between the π MOs of the fragments A and B and the largest π effects are those associated with the interactions π_1–π, π_2–π*, and π–π_3 (see Table 6). These are the only symmetry allowed interactions occurring between the π MOs of the two fragments A and B in the ss and ee conformations. In the se conformations also other interactions can occur, but in all cases the related energy values are found to be negligible. In both *cis*- and *trans*-but-2-enes, the stabilizing interactions π_2–π* and π–π_3 and the destabilizing interaction π_1–π favour the ee over the se and ss conformations and se over ss (there is only the exception of π_2–π* that slightly favours ss over se). The largest contribution is given by the destabilizing effect associated with the π_1–π interaction.

(ii) In all the π interactions occurring in *trans*-but-2-ene, the matrix element and the energy gap operate in the same direction. In *cis*-but-2-enes, this situation is found only in the π–π_3 interaction, while in the π_1–π and π_2–π* interactions the energy gap and the matrix element operate in opposite directions, with the latter being the dominant factor. It is also found that the effect caused by the variations of the energy gaps is very small in all cases, either when the variation of the energy gap tends to reduce the effect of the matrix element or when it tends to reinforce it.

Therefore the results of the quantitative analysis show that

Table 5. Energy effects (kcal mol^{-1}) associated with the relevant [a] σ orbital interactions occurring between fragments A and B (see Scheme 1) in the various conformations of but-2-ene, computed at the STO-3G level

	c_{ss}	c_{se}	c_{ee} [b]	t_{ss}	t_{se}	t_{ee}
$\Delta E^4_{\varphi_1\sigma_{C(1)C(2)}}$	2.97	2.30	2.70 (2.49)	3.50	2.09	2.32
$\Delta E^4_{\varphi_1\sigma_{C(1)H(1)}}$	0.57	0.50	2.99 (2.33)	0.00	0.22	0.99
$\Delta E^4_{\varphi_1\sigma_{C(2)H(2)}}$	0.57	0.93	2.99 (2.33)	0.00	0.71	0.99
$\Delta E^4_{\varphi_2\sigma_{C(1)C(2)}}$	0.00	0.72	0.00 (0.00)	0.00	0.67	0.00
$\Delta E^4_{\varphi_2\sigma_{C(1)H(1)}}$	0.33	3.66	1.70 (1.27)	1.65	3.69	2.52
$\Delta E^4_{\varphi_2\sigma_{C(2)H(2)}}$	0.33	0.00	1.70 (1.27)	1.65	0.34	2.52
$\Delta E^4_{\varphi_3\sigma_{C(1)C(2)}}$	5.64	4.88	4.48 (5.59)	5.94	5.63	7.11
$\Delta E^4_{\varphi_3\sigma_{C(1)H(1)}}$	4.01	1.55	1.79 (1.80)	1.59	2.08	0.05
$\Delta E^4_{\varphi_3\sigma_{C(2)H(2)}}$	4.01	5.17	1.79 (1.80)	1.59	0.21	0.05
$\Delta E^4_{\varphi_4\sigma_{C(1)C(2)}}$	0.00	0.06	0.00 (0.00)	0.00	0.92	0.00
$\Delta E^4_{\varphi_4\sigma_{C(1)H(1)}}$	2.59	1.73	1.47 (1.40)	4.57	1.36	4.84
$\Delta E^4_{\varphi_4\sigma_{C(2)H(2)}}$	2.59	2.18	1.47 (1.40)	4.57	7.87	4.84
$[\Sigma\Delta E^4(\sigma)]_{II}$	23.61	23.68	23.08 (21.68)	24.96	25.79	26.23
$[\Sigma\Delta E^2(\sigma)]_{II}$	−1.90	−1.95	−1.99 (−1.99)	−1.85	−1.96	−2.01
$[\Sigma\Delta E(\sigma)]_{II}$	21.71	21.73	21.09 (19.69)	23.11	23.83	24.22
$\Sigma\Delta E^4(\sigma)$ [c]	25.28	26.25	28.04 (31.54)	24.96	25.79	26.23
$\Sigma\Delta E^2(\sigma)$ [c]	−1.94	−2.06	−2.25 (−2.53)	−1.85	−1.96	−2.01
$\Sigma\Delta E(\sigma)$ [c]	23.34	24.19	25.79 (29.01)	23.11	23.83	24.22

[a] The energy effects associated with the orbital interactions not reported here are, for all conformations, less than |0.1| kcal mol^{-1}. [b] Values in parentheses refer to results obtained in the rigid model with reference to t_{ee}. [c] $\Sigma\Delta E(\sigma) = [\Sigma\Delta E(\sigma)]_I + [\Sigma\Delta E(\sigma)]_{II}$ {$[\Sigma\Delta E(\sigma)]_I$ given in Table 4}.

Table 6. Energy effects (kcal mol^{-1}) associated with the π orbital interactions occurring between fragments A and B (see Scheme 1) in the various conformations of but-2-ene, computed at the STO-3G level

	c_{ss}	c_{se}	c_{ee} [a]	t_{ss}	t_{se}	t_{ee}
$\Delta E^4_{\pi\pi_1}$	29.61	28.98	28.57 (28.01)	29.89	29.17	28.05
$\Delta E^4_{\pi\pi_2}$	0.00	0.00	0.00 (0.00)	0.00	0.31	0.00
$\Delta E^2_{\pi\pi_3}$	−3.25	−3.24	−3.43 (−3.59)	−2.84	−3.26	−3.63
$\Delta E^2_{\pi\pi_4}$	0.00	0.00	0.00 (0.00)	0.00	−0.01	0.00
$\Delta E^2_{\pi_1\pi^*}$	0.00	0.00	0.00 (0.00)	0.00	−0.07	0.00
$\Delta E^2_{\pi_2\pi^*}$	−5.94	−5.88	−6.10 (−5.84)	−5.39	−5.48	−5.74
$[\Sigma\Delta E^4(\pi)]_{II}$	29.61	28.98	28.57 (28.01)	29.89	29.48	28.05
$[\Sigma\Delta E^2(\pi)]_{II}$	−9.19	−9.12	−9.53 (−9.43)	−8.23	−8.82	−9.37
$[\Sigma\Delta E(\pi)]_{II}$	20.42	19.86	19.04 (18.58)	21.66	20.66	18.68
$\Sigma\Delta E^4(\pi)$ [b]	30.11	29.04	28.58 (28.03)	29.89	29.48	28.05
$\Sigma\Delta E^2(\pi)$ [b]	−9.25	−9.13	−9.53 (−9.43)	−8.23	−8.82	−9.37
$\Sigma\Delta E(\pi)$ [b]	20.86	19.91	19.05 (18.60)	21.66	20.66	18.68

[a] Values in parentheses refer to results obtained in the rigid model with reference to t_{ee}. [b] $\Sigma\Delta E(\pi) = [\Sigma\Delta E(\pi)]_I + [\Sigma\Delta E(\pi)]_{II}$ {$[\Sigma\Delta E(\pi)]_I$ given in Table 4}.

the factors which favour eclipsed over staggered propene also control the trend of the energy effect associated with the π non-bonded interactions not only in the three *trans*-conformations, but also in the three *cis*-ones.

On the other hand, the analysis of the σ orbital interactions reveals that (i) the energy effects associated with the σ orbital interactions occurring between the two CH_3 fragments (see Table 4) are found to be negligible in the *trans*-conformations, but significant in the *cis*-ones, where in each conformation only one interaction is found to be relevant, *i.e.* φ–φ′ in c_{ss}, φ–σ′$_{CH}$ in c_{se}, and σ$_{CH}$–σ′$_{CH}$ in c_{ee}. The order of the related destabilizing effect is $\Delta E^4_{\varphi-\varphi'} < \Delta E^4_{\varphi-\sigma'_{CH}} < \Delta E^4_{\sigma_{CH}-\sigma'_{CH}}$ and parallels the trend of the total energy affect associated with the σ orbital interaction $\Sigma\Delta E(\sigma)$.

(ii) The energy effects associated with the relevant σ interactions between fragments A and B are listed in Table 5. To understand their effect, it is convenient to compare the following two contributions: (i) the energy effect associated with the interaction of the various σ orbitals of the CH_3 fragments with the C–C bond MO of the ethylene fragment and (ii) the energy effect associated with the interactions occurring between the σ MOs of the CH_3 fragments and the σ$_{CH}$ MOs of the ethylene fragment. In both *cis*- and *trans*-butenes, the latter energy effect, which is destabilizing, favours the ss over the se and the se over the ee conformation: this trend is determined by interactions involving the φ MOs of the CH_3 fragments. On the other hand the former energy effect has similar values in the *trans*-conformations, so that in *trans*-but-2-ene the overall σ energy effect follows the order ee > se > ss. However, in the *cis*-conformations the former energy effect favours the ee over the se and the se over the ss conformation. This effect can be considered to be a manifestation of σ aromaticity, but is not large enough to counterbalance the effect of the steric repulsions between the σ MOs of the CH_3 fragments and the σ$_{CH}$ MOs of the ethylene fragment and between the σ MOs of the two CH_3 fragments, which both favour the ss over the se and the se over the ee conformation.

We have also estimated the values of the Coulomb energy (E_c) associated with the interaction of the three fragments, according to equation (5). Using the net atomic charges obtained from the Mulliken population analysis, the computed E_c values (kcal mol^{-1}) have been found to be 1.22 in c_{ss},

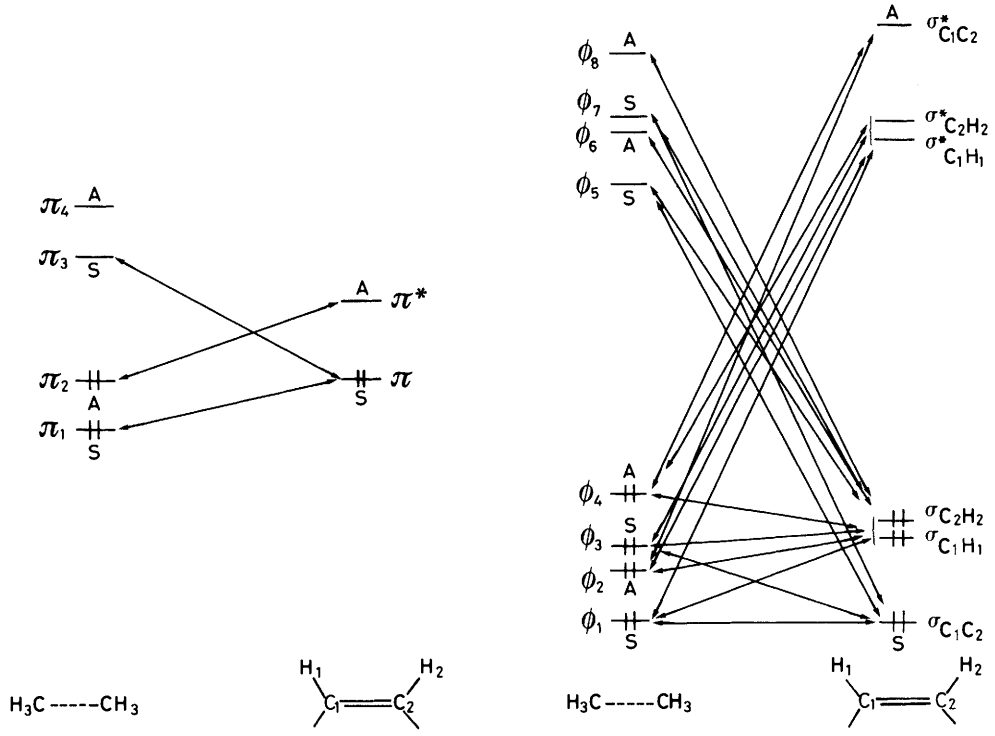

Figure 4. Interaction diagram between the MOs of fragments A and B in but-2-ene (A, π interactions, B, σ interactions)

Table 7. Methyl rotational barriers in propene and but-2-ene

Compound	Transformation	Experimental (kcal mol^{-1})	Computed values 4-31G A [d]	4-31G B [e]	STO-3G A [d]	STO-3G B [e]
Propene	Eclipsed ⟶ Staggered	2.00 [a]	1.820		1.537	
But-2-ene	c_{ee} ⟶ c_{se}	0.45—0.7 [b]	0.452	1.017	0.333	0.627
	t_{ee} ⟶ t_{se}	1.95 [c]	1.826	1.776	1.550	1.537
	c_{se} ⟶ c_{ss}		0.539	1.280	0.477	0.897
	t_{se} ⟶ t_{ss}		1.908	1.518	1.600	1.362

[a] See ref. 12. [b] See refs. 17 and 18. [c] See ref. 18. [d] Rotational barriers at the SCF level. [e] Rotational barriers in the absence of the π interactions between a methyl group and the adjacent propene-like fragment.

1.19 in c_{se}, 1.20 in c_{ee}, 1.12 in t_{ss}, 1.11 in t_{se}, and 1.10 in t_{ee}. These results show that this term has a negligible effect upon the conformational preference.

Methyl Rotational Barriers in But-2-ene.—Experimentally it is found that the rotational barrier of the methyl group in *trans*-but-2-ene is of the order of magnitude of that in propene, while that in *cis*-but-2-ene is significantly smaller (see Table 7). The barrier to methyl rotation in *cis*-but-2-ene is the energy difference between the c_{ee} and c_{se} conformations with c_{ee} being an energy minimum and c_{se} an energy maximum. Similarly, the methyl rotational barrier in *trans*-but-2-ene is the energy difference between the t_{ee} and the t_{se} conformations with t_{ee} being the energy minimum and t_{se} the energy maximum.

In order to assess quantitatively the effect of the π non-bonded interactions upon the rotational barrier, we have made use of the Total Energy approach with the dissection shown in Scheme 2 that gives the values of the rotational barrier in the absence of π interactions between a methyl group and the adjacent propene-like fragment.

We then computed the corresponding total energy values in the absence of these interactions and the computed rotational barriers with and without these π interactions are listed in Table 7. We report here also the values computed for the se ⟶ ss transformations. We also repeated the computation of the rotational barriers with and without these π interactions at the 4-31G level [16] and the results are also listed in Table 7. It can be seen that both computational levels provide values of the rotational barriers which agree well with the experimental data [17,18] even if the 4-31G values seem to be slightly more accurate. At both computational levels the *trans*-rotational barriers are almost identical to the corresponding values for propene, while both *cis*-barriers are significantly smaller.

The values computed in the absence of the π non-bonded interactions show that the effect of such interactions is very small in the *trans*-barriers, as expected. On the other hand, in the *cis*-geometries, the effect of these interactions is more significant and such as to decrease the rotational barrier. However both the *cis*-barriers computed in the absence of these interactions are still significantly smaller than the value in propene, indicating that the σ non-bonded interactions play a

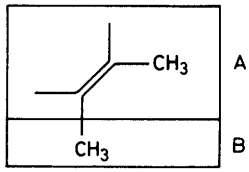

Scheme 2

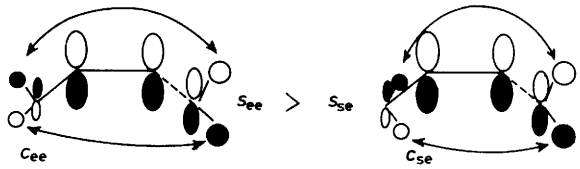

Scheme 3

significant role in determining the decrease in the magnitude of the *cis*-barriers.

The analysis of the various results provide additional information about the effects mainly responsible for these trends in the *cis*-geometries. In particular it is found that (i) the effect of the π interactions occurring between the π MOs of a methyl group and those of a propene-like fragment is more destabilizing when the propene-like fragment adopts an eclipsed conformation. This trend is mainly caused by the variation of the energy effect associated with the orbital interaction involving the π HOMOs of the two interacting fragments and illustrated in Scheme 3 for the $c_{ee} \longrightarrow c_{se}$ transformation. As can be seen, there is an increase in the antibonding overlap between the methyl hydrogens in going from c_{ee} to c_{se} which effectively reduces the total overlap integral in the c_{se} geometry and consequently the destabilization energy associated with this orbital interaction. For similar reasons this interaction will favour c_{ss} over c_{se}; furthermore, in this case, the effect is more pronounced since the variation in the overlap integral is more significant because of the smaller distance between the methyl hydrogens.

(ii) The σ non-bonded interactions which play a major role are those occurring between the two methyl groups, *i.e.* φ–φ′ in c_{ss}, φ–σ′$_{CH}$ in c_{se}, and σ_{CH}–σ′$_{CH}$ in c_{ee}. As previously pointed out, the destabilizing effect of these interactions follows the order $\Delta E^4_{\varphi-\varphi'} < \Delta E^4_{\varphi-\sigma'_{CH}} < \Delta E^4_{\sigma_{CH}-\sigma'_{CH}}$: consequently c_{ee} is destabilized with respect to c_{se}, and the latter with respect to c_{ss}. Therefore, the σ effect destabilizes the energy minimum more: furthermore, because the energy minimum c_{ee} is more destabilized than c_{se} with respect to the corresponding energy maxima, the barrier for the $c_{ee} \longrightarrow c_{se}$ transformation is smaller than that for the $c_{se} \longrightarrow c_{ss}$ one.

Geometrical Isomerism of But-2-ene.—The discussion about the geometrical isomerism in but-2-ene is based on a comparative analysis of the two most stable *trans*- and *cis*-conformers, *i.e.* t_{ee} and c_{ee}. At the STO-3G level, the t_{ee} conformer is found to be more stable than c_{ee} by 3.20 kcal mol^{-1} in the rigid model and by 1.89 kcal mol^{-1} in the optimized model, in agreement with the experimental observations.[19]

In the absence of the π interactions (see Table 3), the t_{ee} conformer remains more stable than c_{ee} in both models and also the relative stabilities remain of similar order of magnitude (3.27 kcal mol^{-1} in the rigid model and 1.40 kcal mol^{-1} in the optimized model). These results suggest that the π non-bonded interactions play only a minor role in determining the relative stability of the two most stable *cis*- and *trans*-conformers, and that this problem is dominated by the σ non-bonded interactions.

More detailed information is provided by the quantitative PMO analysis. We discuss first the results obtained in the rigid model, which agree very well with the indications of the Total Energy approach. It is found, in fact, that while the overall energy effect associated with the π interactions, $\Sigma\Delta E(\pi)$ in Table 6, is of the same order of magnitude in the two geometries, the overall energy effect associated with the σ interactions, $\Sigma\Delta E(\sigma)$ in Table 5, is less destabilizing in the t_{ee} than in the c_{ee} geometry. The analysis of the component terms reveals that the effect of the π orbital interactions, either destabilizing or stabilizing, is about the same in the two geometries, while the effect of the σ orbital interactions $\Sigma\Delta E(\sigma)$ is dominated by the destabilizing contribution $\Sigma\Delta E^4(\sigma)$. This trend is determined by the effect associated with the σ orbital interactions between the two methyl groups, $[\Sigma\Delta E(\sigma)]_I$ (see Table 4), and in particular by the term $\Delta E^4_{\sigma_{CH}-\sigma'_{CH}}$, *i.e.* the repulsion between the two in-plane σ_{CH} bond MOs of the methyl groups. This interaction is, in fact, very large in c_{ee} and negligible in t_{ee} and constitutes the largest differential contribution to the steric effect. On the other hand, the energy effect associated with the σ interactions between the fragments A and B, $[\Sigma\Delta E(\sigma)]_{II}$ in Table 5, favours c_{ee} over t_{ee}: this effect can be considered a manifestation of σ aromaticity, which, however, is dominated by steric effects, as previously pointed out.[5]

The comparison with the results obtained in the optimized model shows that the geometry relaxation of the c_{ee} isomer has the effect mainly of reducing the repulsion between the σ_{CH} bond MOs through an increase of the α and β angles [5] (α from 109.7 to 111.2° and β from 124.6 to 126.9°). In this way, the overall energy effect $\Sigma\Delta E$ becomes significantly less destabilizing than in the c_{ee} rigid geometry, but still slightly more destabilizing than in the t_{ee} geometry. As previously pointed out,[1,2] this reduction of the destabilization energy is obtained at the expense of a destabilization of various fragment localized MOs, in particular here the σ_{CH} bond MOs.

Conclusions.—We have presented a detailed quantitative analysis of the effects of σ and π non-bonded interactions in but-2-enes and have reached the following conclusions.

(i) The relative conformational stabilities in both *cis*- and *trans*-but-2-ene, ee > se > ss, are determined by the same factors which favour eclipsed over staggered propene, *i.e.* the π non-bonded interactions under matrix element control. This report partly contradicts the conclusions of qualitative analysis [5] where it was suggested that the conformational preferences are controlled in *trans*-but-2-ene by the π non-bonded interactions and in *cis*-but-2-ene by σ aromaticity and nuclear–nuclear repulsions.

(ii) The decrease in the magnitude of the rotational barrier in *cis*-but-2-ene, compared with that in *trans*-but-2-ene, is determined by effects associated with both the σ and π interactions between the two methyl groups, which preferentially destabilize the energy minimum.

(iii) The relative stability of the two geometric isomers, $t_{ee} > c_{ee}$, is determined mainly by the steric repulsions between the σ_{CH} bond MOs of the two methyl groups, which are large in c_{ee} and negligible in t_{ee}. This conclusion agrees with the results of qualitative analysis,[5] but is in contrast with the results of Wolfe *et al.*,[6] who have attempted to rationalize this trend in terms of π effects only.

(iv) The electrostatic interactions between the various fragments have been found to have a negligible effect in the torsional problems under examination.

References

1 F. Bernardi and A. Bottoni, *Theor. Chim. Acta*, 1981, **58**, 245.
2 F. Bernardi and A. Bottoni, in R. Daudel and I. G. Csizmadia, 'Computational Theoretical Organic Chemistry,' Reidel, 1981.
3 R. Hoffmann, *Acc. Chem. Res.*, 1971, **4**, 1.
4 N. D. Epiotis, *J. Am. Chem. Soc.*, 1973, **95**, 3087.
5 N. D. Epiotis, R. L. Yates, and F. Bernardi, *J. Am. Chem. Soc.*, 1975, **97**, 5691.
6 S. Wolfe, D. J. Mitchell, and M. H. Whangbo, *J. Am. Chem. Soc.*, 1978, **100**, 1936.
7 W. J. Hehre, R. F. Stewart, and J. A. Pople, *J. Chem. Phys.*, 1969, **51**, 2657.
8 J. S. Binkley, R. A. Whiteside, P. C. Hariharan, R. Seeger, and J. A. Pople, *QCPE*, 1978, **11**, 368.
9 F. Bernardi, M. A. Robb, and G. Tonachini, *Chem. Phys. Lett.*, 1979, **66**, 195.
10 N. C. Baird and R. M. West, *J. Am. Chem. Soc.*, 1971, **93**, 4427; K. Müller, *Helv. Chim. Acta*, 1970, **53**, 1112.
11 See E. Heilbronner and H. Bock, 'Das HMO-Modell und Seine Annendung,' Verlag Chemie, Weinheim, 1968; M. J. S. Dewar, 'The Molecular Orbital Theory of Organic Chemistry,' McGraw-Hill, New York, 1969.
12 E. Hirota, *J. Chem. Phys.*, 1966, **45**, 1984; W. G. Fotely and F. A. Miller, *Spectrochim. Acta*, 1963, **19**, 611; K. D. Moller, A. R. De Meo, D. R. Smith, and L. H. London, *J. Chem. Phys.*, 1967, **47**, 2609.
13 M. H. Whangbo, H. B. Schlegel, and S. Wolfe, *J. Am. Chem. Soc.*, 1977, **99**, 1296.
14 W. J. Hehre and L. Salem, *J. Chem. Soc., Chem. Commun.*, 1973, 754.
15 N. D. Epiotis, W. Cherry, S. Shaik, R. L. Yates, and F. Bernardi, *Top Curr. Chem.*, 1977, **70**, 66.
16 R. Ditchfield, W. J. Hehre, and J. A. Pople, *J. Chem. Phys.*, 1971, **54**, 724.
17 T. N. Sarachman, *J. Chem. Phys.*, 1968, **49**, 3146.
18 J. E. Kilpatrick and K. S. Pitzer, *J. Res. Nat. Bur. Stand.*, 1946, **37**, 163.
19 F. D. Rossini, K. S. Pitzer, R. L. Arnett, R. M. Braun, and G. C. Pimental, 'Selected Values of Physical and Thermodynamic Properties of Hydrocarbons and Related Compounds,' American Petroleum Institute Research Project No. 44, Pittsburgh, 1953.

Received 15*th March* 1982; *Paper* 2/445